# Morphology and properties of the graphene layer on the copper substrate

**Katarzyna Pietrzak, Wiesława Olesińska, Cezary Strąk, Robert Siedlec[*], Andrzej Gładki**

*Institute of Electronic Materials Technology, Wólczyńska 133, 01-919 Warsaw, Poland*
[*]Corresponding author: e-mail: robert.siedlec@itme.edu.pl

The aim of the work presented in the article was to clarify controversial comments about anti-corrosion and mechanical properties of graphene coatings, deposited on copper substrates. It was designed special experimental cycle comprising: preparation of graphene forms and copper, the observation of layers Cu / GO (rGO) after the thermal reduction processes and oxidative test in air at 150°C temperature and 350 h in time. The resulting coatings and graphene layers were subjected to tribological test for hardness. The observed differences in the continuity of the coverage copper surface by graphene forms, allowed to understand the macroscopic effect of increased hardness and wear resistance layers rGO/Cu.

**Keywords:** copper, graphene, graphene oxide, reduced graphene oxide.

## INTRODUCTION

The results of numerical simulation of noble gases diffusion, oxygen, nitrogen[1–2] by a single layer of graphene, obtained by DFT[3] (Density Functional Theory) indicate that graphene is impermeable material. This opinion is expressed quite categorically – *Graphene has been shown to provide an impermeable barrier; its surface forms a natural diffusion barrier, and provides physical isolation between the metal and the reactant*[2]. In some sense, this fact is confirmed by the results of experiments performed on the graphene microdrum[4]. The results indicate a negligible diffusion of He, Ar and air, at zero differential pressure on both sides of the graphene drumhead. Taking into account the results of DFT method, should be considered a very important element. The results of this method of calculation relate is to the basic state of matter, defined as one in which power an increase over time is zero, or the Hamiltonian of the system is independent in time. Generally, refer to relaxed, isolated systems. Hence, among other things, many hours of relaxation periods described graphene drum[4]. The presence of isolated systems in nature is unlikely and very difficult or impossible in theoretical description, when Hamiltonian of the system changes in time. In such cases, experience is the best description of the phenomenon. In the case of graphene, in real CVD (Chemical Vapor Deposition) conditions, graphene is no significant diffusion barriers to Li or Na atoms[5]. Graphene oxide, which is under a pressure of 100 mbar practically impermeable to He, H, N and Ar, is water permeable under low hydrostatic pressure[6]. This phenomenon has been extensively discussed in the publication[7]. The impermeability of the graphene has stimulated research into the use of this material to protect others from the activities of external factors. Commercially reasonable are researches on the creation of slight graphene anticorrosion, antioxidant coatings on copper. Anticorrosion coating graphene perfectly protect copper electrochemical cells[8–9]. On antioxidant graphene coatings opinions are divided. Very good antioxidant results of coatings obtained for epitaxial graphene on copper are shown in publication[10]. However, conclusion of publication[11] indicating the acceleration of oxidation of copper, coated with graphene obtained by CVD. These disparities have become the impulse to carry out their own studies, involving observation of the oxygen migration from zones rich in this element to impoverished areas. Two groups of experiments were designed. In the first group, intentionally oxidized copper surface, had covered with slurry: reduced graphene oxide (rGO) in isopropanol alcohol. Isopropanol is a very good graphene dispersant and graphene impermeable it[6]. The second group consisted of deoxygenated copper substrate coated with an oxygen-rich aqueous solution of graphene oxide (GO). An aqueous solution of graphene oxide was obtained directly from a chemical process manufacturing it. The samples from both groups have been reduced in nitrogen atmosphere at identical thermal conditions. Studies have been analyzed in a wide range microscopy – from optical to high resolution scanning electron microscopy. Continuity of graphene coatings were investigated by Raman spectroscopy mapping. Oxidative test layers were carried out in air atmosphere at the time of 350 h and 150°C temperature.

## EXPERIMENT

The following basic materials were used in this experiment:
– polycrystalline, copper foil (M00B), 0.15 mm in thick,
– aqueous solution of graphene oxide (GO) and thermally reduced graphene oxide (rGO) dispersed in isopropyl alcohol. Both GO, rGO coming from: Department of Chemical Technology/ITME.

Diagram of the experiment is shown in Figure 1. In the first stage of experiment all copper substrates were annealed at a temperature of 700°C in nitrogen atmosphere (stage 1 in Fig. 1). Next, part of the substrates was oxidized in air at a temperature of 250°C (stage 2 in Fig. 1). SEM images of copper surfaces, after both stages 1 and 2 are shown in Figure 2. Images of both surface are completely different. The oxidized copper surface is outspreading, consist of granules of copper oxide. Granular structure with highly outspreading grains with diameter of around 200 nm suggests that high adhesive forces linked with capillary pressure can be expected. Copper with deoxidized surface (Fig. 2b) is a set of planes typical for intragranular crystallization and steps dislocation in copper grain boundaries. In the third stage of the experiment, the prepared copper surfaces were covered with graphene oxide slurries. Alcoholic
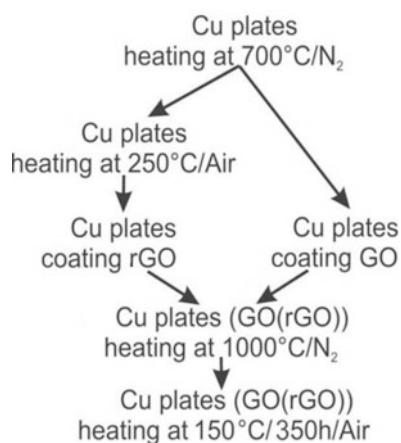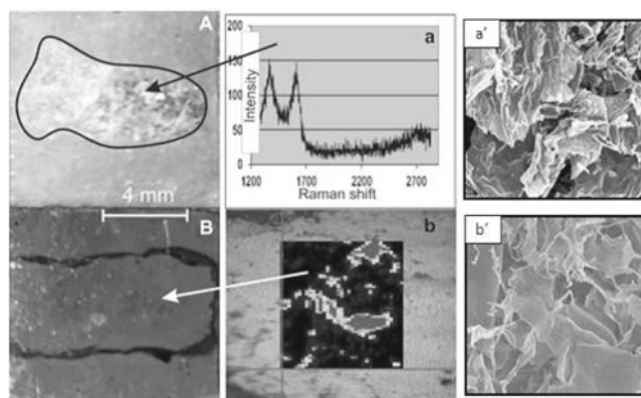
**Figure 1.** Diagram presenting the experiment
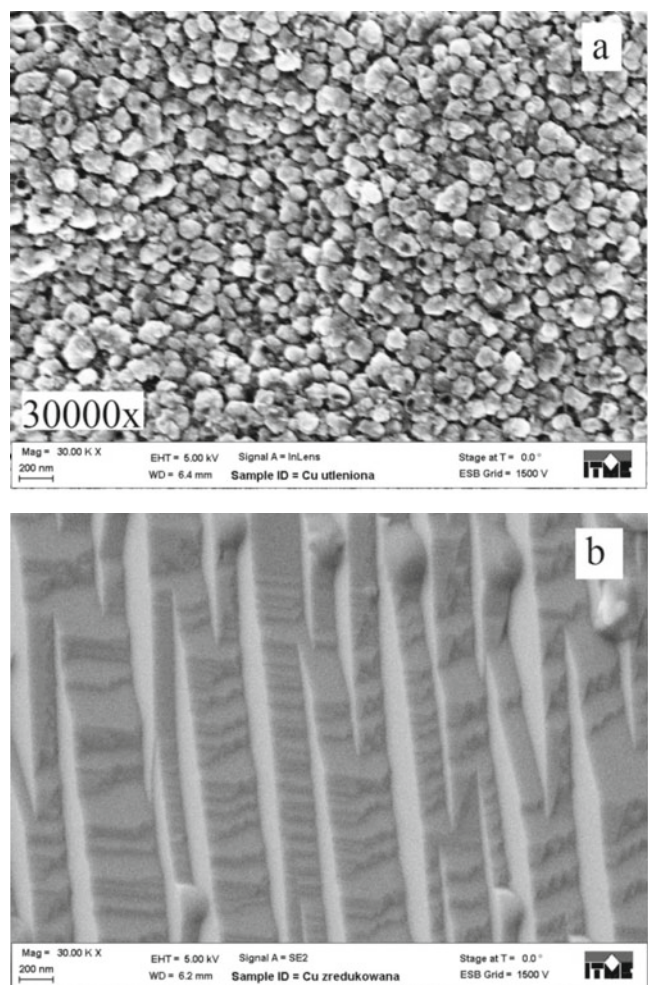


**Figure 2.** SEM image of the surface of copper thermal processes after: a) oxidation at 250°C. b) reduction of an oxide layer in nitrogen atmosphere containing around 1.5 ppm of oxygen at 1000°C



**Figure 3.** A) Sample of intentionally oxidized copper with a layer of rGO (inside of the outline) after annealing at T = 1000°C/N$_2$; B) sample of copper coating by GO after identical thermal treatment; a) Raman spectrum typical inside of the contour in A); b) map of discontinuities of Raman spectrum for graphene forms in the area of the Cu/GO coating marked in B), a') SEM image of rGO, b') SEM image of GO

solution of rGO was applied onto the surface of oxidized copper. The surface of deoxidized copper was covered with water solution of GO. When the solvents dried, the coatings samples were annealed at 1000°C in nitrogen atmosphere. SEM images of dry GO and rGO forms (Fig. 3a', b') and macro photographs of copper wafers the fourth stage after were shown in Figure 3A, B.

Macroscopic observation of the intentionally oxidized surface of copper with a layer of rGO indicated the presence of oxidation outside the contour presented in Figure 3A. Oxidation was unobservable inside the contour and the covering of rGO on the surface was clearly visible in Raman spectroscopy (Renishaw – InVia Raman Microscope) (Fig. 3a). Similar observation of the surface of deoxidized copper GO coating (Fig. 3B) no showed surface changes, the annealing process after. A local Raman spectroscopy analysis did not confirm the presence of any graphene forms in the analyzed area. On the other hand, planar analysis of a Raman spectrum (Fig. 3a) showed, that graphene oxide discontinuous covered copper. Red color in Fig. 3b represents the maximum intensity for the GO coating, while the copper substrate is in black. Outside area of map, local pink spots of oxidized copper (Cu$_2$O) are visible. Their confirms discontinuously covering copper by graphene oxide and is the proof that only GO can be the source of oxygen. At the final, fifth step of this experiment both types of the prepared substrates to atmospheric oxygen were exposed. The samples were annealed in air atmosphere at 150°C for 350 hours, treating this stage of the experiment as a test of resistance of graphene coatings to copper oxidation.

**RESULTS**

Abrasion and hardness tests were performed for both types of copper surface coatings. The following parameters were kept constant in tribological tests (Nanotribometr NRT2 – CSM Instrumrnts): an indenter – a ball 2 mm in diameter made of 100 Cr6 steel, load of 100 mN, maximum rubbing speed of 2 cm · s$^{-1}$. The results of wear tests are presented in Table 1, while profilograms of ball traces and the degree of its wear can be found in Figure 4.

The analysis of wear profilograms, ball geometry and numerical results clearly shows the hierarchy of values of the friction coefficient $\mu$ as monotonic: $\mu$(Cu)>$\mu$(Cu/GO)>$\mu$(Cu/rGO). The sequence of the friction coefficients in this set proves that the Cu surface, modified rGO, had a higher wear resistant. The wear results coincide with the hardness results (Hardness tester – DuraScan 10 Struers), when average hardness values are in a

**Table 1.** Results of fifteen wear tests performed for the samples: a – native copper substrate; b – surface of oxidized copper covered with rGO; c – surface of deoxidized copper covered with GO

| No. | Coefficient of friction | | Wear traces [μm2] | | Wear diameter ball [μm] | |
|---|---|---|---|---|---|---|
| | Average | Standard deviation | Average | Standard deviation | Average | Standard deviation |
| a | 0.57 | 0.13 | 134.5 | 50.8 | 81.5 | 20.4 |
| b | 0.33 | 0.11 | 53.4 | 35.5 | immeasurable | immeasurable |
| c | 0.39 | 0.08 | 104.8 | 19.8 | 85.0 | 21.2 |
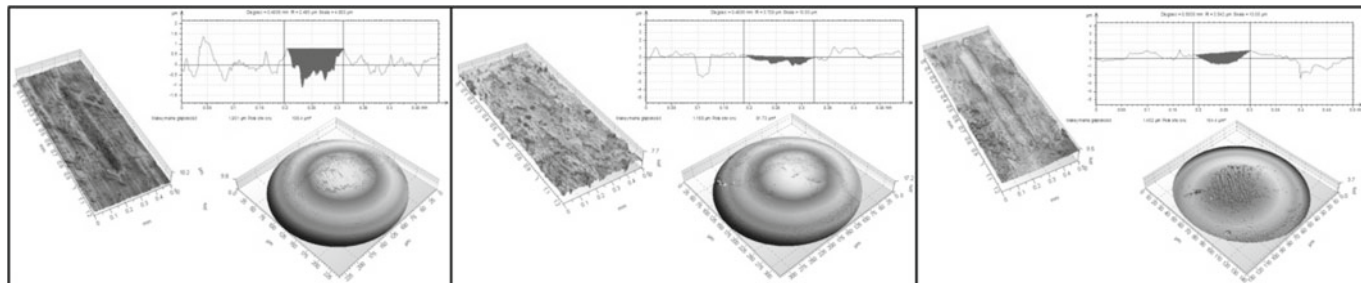


**Figure 4.** Images of wear traces for the substrate and ball, a – Cu; b – Cu/Cu$_2$O  rGO; c – Cu-GO

decreasing sequence 80HV0.01(Cu/rGO)>49HV0.01(Cu/GO)≥47HV0.01(Cu).

Using the SEM-EBSD method (Electron BackScattering Diffraction) the oxidation degree of the prepared copper surfaces, exposed for a long time to atmospheric, was analyzed. Figure 5 shows binary maps representing copper and its oxides: Figure 5a – pure copper, Figure 5b – Cu modified GO, Figure 5c – Cu modified rGO. The red color of binary maps represents of pure copper, whereas tenorite is marked with green and Cu$_2$O with blue. Binary SEM-EBSD black color has been assigned to unidentified quality. The percentage of copper and its oxides, estimated SEM-EBSD method are collated in Table 2.

The analysis of images and data shown in Figure 5 and Table 2 indicated that copper covered with rGO a layer

**Table 2.** The results of EBSD analysis obtained for the studied surfaces

| Material | | Percentage [%] | | |
|---|---|---|---|---|
| | | Cu/Cu$_2$O−rGO | Cu−GO | Cu |
| Copper | | 63.8 | 22.55 | 23.15 |
| CuO tenorite | | 13.7 | 58.60 | 56.35 |
| Cu$_2$O | | 22.5 | 18.85 | 20.50 |

is definitely more resistant to oxidation than copper coated with GO. In addition, no significant differences are observed in the composition of oxides, decorating the surface of both pure copper and copper covered with GO. This means that only rGO coatings Cu get anticorrosive surface properties. When seeking mechanism explaining high anticorrosive efficiency of rGO, Cu/rGO near-surface layers were studied using high-resolution electron microscopy methods (HRTEM). The investigation into the near-surface areas carried out employing various HRTEM techniques revealed the presence of a mixture of Cu$_2$O oxides with different orientations.
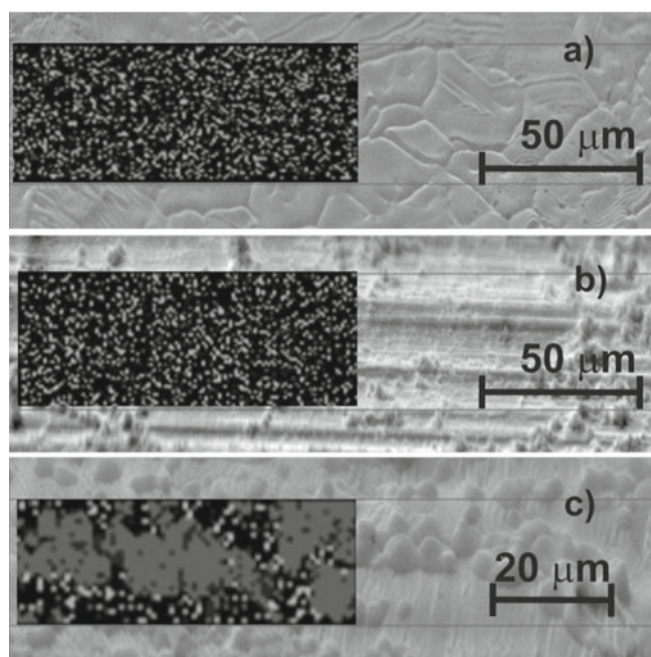


**Figure 5.** SEM images of the copper surface and EBSD maps of chemical elements distribution in marked areas after oxidation in air atmosphere, lasting 350 hours: a) oxygen-pure copper, b) oxygen-pure copper with a layer of GO, (copper was marked with grey, carbon with dark grey and oxygen with light grey), c) oxidized copper with a layer of rGO
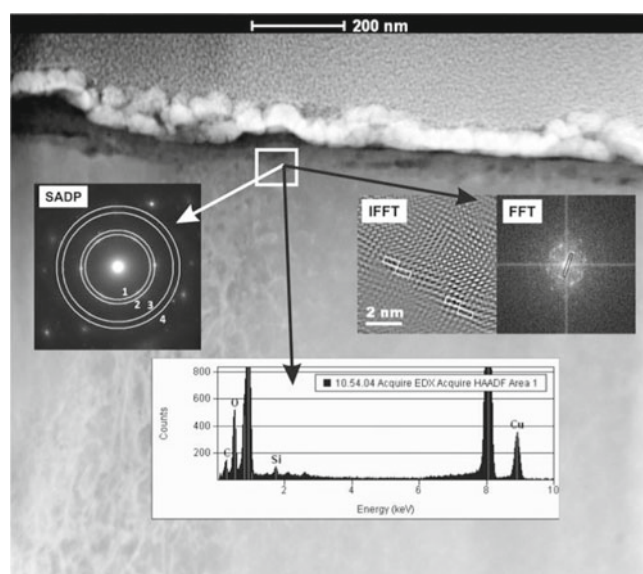


**Figure 6.** High-resolution electron microscopy images showing the presence of copper oxide and copper (white square) in the boundary layer: Cu$_2$O having different orientations (SADP); dispersed graphene forms (IFFT, FFT); Cu, O, C (EDX) chemical compounds

The following orientations are identified in the SADP image in Figure 6: [111] circle 1; [020] circle 2; [202] circle 3; [311] circle 4. IFFT and FFT techniques clearly indicate the presence of fine graphene forms built-in the structure of Cu-Cu$_2$O. The presence of carbon in the near-surface layer is confirmed by the EDX HAADF field analysis. A similar, complete HRTEM analysis of the copper surface covered with GO did not reveal any carbon, but only a thick layer of oxides.

A bright fibrous structure, visible in Figure 6, consisting of dislocation bands in copper. Most probably, that these dislocations were propagated in the pristine plastic forming of copper foils. A great number of mouth dislocation is particularly visible on the copper surface covered with rGO. The SEM EDS analysis of mouth dislocation on the surface, indicates the predominance of pure copper with traces of its oxides (Fig. 7). There are no similar mouth dislocation in images of the pure copper samples and copper coated with GO. It suggests, that rGO built-in into the near-surface layer decreases potential of surface energy, facilitating migration of dislocations during annealing processes. Perhaps, that the movement of dislocations stimulates the transport of mass from the near-surface Cu-Cu2O/rGO layer, lifting oxides to the surface.
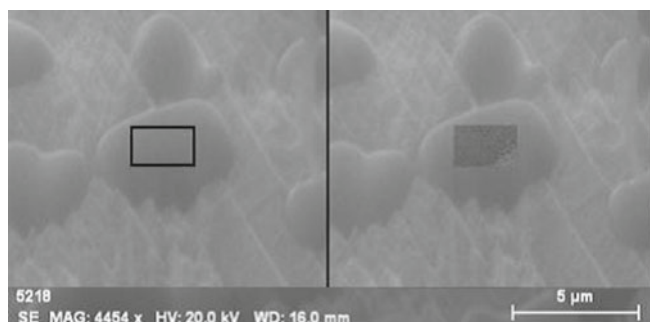


**Figure 7.** SEM image and EBSD map of chemical elements distribution for inclusions on the surface of copper, formed after oxidation (copper was marked with grey, carbon with dark grey and oxygen with light grey)

## SUMMARY

A transport mechanism of oxygen, which transforms native rGO coatings on copper – Cu/rGO – into thin Cu(Cu$_2$O)rGO layers and leaves Cu/GO coatings as discontinuous island centers of thermally reduced native GO, arises from the analysis of the research works performed. High-resolution structural HRTEM measurements demonstrate it. This hypothesis is confirmed by tribological and hardness tests, showing higher hardness and wear resistance for the native Cu/rGO, coating thermally transformed into the Cu(Cu$_2$O)rGO layer. The native Cu/GO coating remains only a set of areas of thermally reduced GO, loosely bonded to the surface of copper, hence its lower wear resistance and hardness for pure copper. The oxygen transport process is explained in Figure 8. The diagram assumes an uneven amount of oxygen in both graphene oxide forms. It is obvious that the fraction of oxygen in GO is higher than in the case of thermally reduced graphene oxide rGO – $O_2(GO) > O_2(rGO)$. Comparing oxygen in pure copper and oxidized copper is a trivial dependence: $O_2(Cu_2O; CuO) >> O_2(Cu)$. In accordance with the essence of chemical potentials, the energy of the annealing process
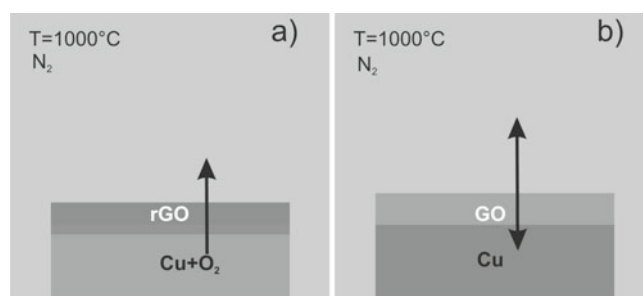


**Figure 8.** Diagram presenting the preparation process of the studied samples

at 1000°C releases oxygen from structures richer in it to areas poor in oxygen. For that probably, deoxidation of the Cu$_2$O layer, its structural transformation process with rGO and emission of oxygen–depleted layer are observed. In the case of the GO coating, thermally oxygen disengagement from it penetrates the GO structures, reducing itself to rGO. The penetrates can be seen as copper coating discontinuities. At the same time, oxygen is bonded to pure copper and transmitted is to the N$_2$ atmosphere. As a result, one observes oxidized copper areas, which should be treated as discontinuous coatings of the native GO layer. The transmission mechanism of oxygen through thermally reduced graphene oxide as such is one missing link in the diagram presented in Figure 8. A planar projection of copper and graphene unit cells in a real size scale is presented in Figure 9.
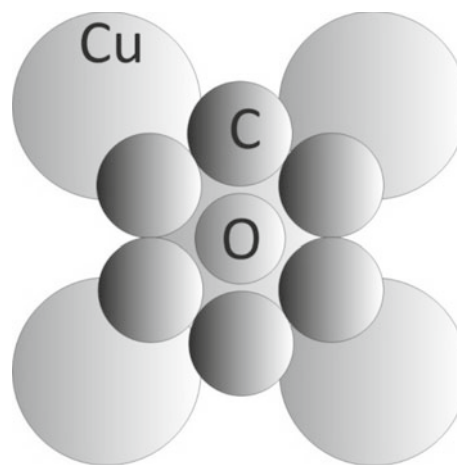


**Figure 9.** Metrically scaled copper, graphene and oxygen elementary cells

The diameter of the oxygen atom is smaller than the graphene lattice. That is why, the oxygen atom with a given kinetic energy can freely penetrate the copper cell. On the other hand, kinetic energy has to be higher than the potential barrier of the system of energetically self-consistent copper and graphene lattices. When graphene lattices create an assembly of a few surfaces (Fig. 10), the connection boundary of Cu-rGO becomes three-dimensional. The energy of the oxygen atom passing through a multi-layer rGO structure has to be so high as to overcome the potential of the graphene lattice alone. This effect is shown graphically in Figure 10 as the covering of copper cells achieved by applying two graphene layers on top. As consequence, at higher temperatures deoxidation of the copper surface covered with rGO is possible, whereas at lower temperatures it becomes a barrier for oxygen.
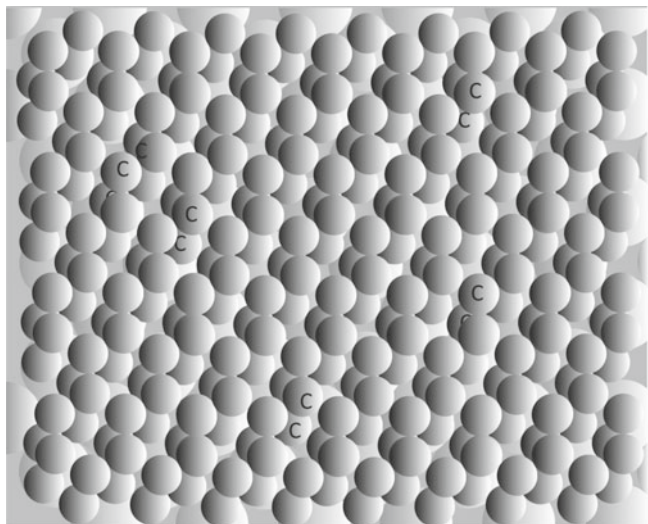
**Figure 10.** Diagram presenting the shape of graphene and copper lattices – two shifted graphene layers

## LITERATURE CITED

1. Leenaerts, O., Partoens, B. & Peeters, F.M. (2008). Graphene: a perfect nanoballoon, *Appl. Phys. Lett.* 93, 193107. DOI: 10.1063/1.3021413.

2. Tsetseris, L. & Pantelides, S.T. (2013). Graphene: An impermeable or selectively permeable membrane for atomic species? *Carbon* Vol. 67, 58–63. DOI: 10.1016/j.carbon.2013.09.055.

3. Cuevas, J.C. (2010). Introduction to Density Functional Theory, https://www.uam.es/personal_pdi/ciencias/jcuevas/Talks/JC-Cuevas-DFT.pdf

4. Bunch, J.S., Verbridge, S.S., Alden, J.S., Arend, M. van der Zande, Parpia, J.M., Craighead, H.G. & McEuen, P.L. (2008). Impermeable Atomic Membranes from Graphene Sheets, NANO LETTERS, Vol. 8, No. 8, 2458–2462. DOI: 10.1021/nl801457b.

5. Boukhvalov, D.W. & Virojanadara, C. (2012). Penetration of alkali atoms throughout a graphene membrane: theoretical modeling, *Nanoscale* 4, 1749–1753. DOI: 10.1039/C2NR11892K.

6. Nair, R.R., Wu, H.A., Jayaram P.N., Grigorieva, I.V. & Geim A.K. (2012).Unimpeded Permeation of Water Through Helium-Leak–Tight Graphene-Based Membranes, *Sci.,* Jan 27, Vol. 335, No. 6067, 442–444. DOI: 10.1126/science.1211694.

7. Boukhvalov, D.W. & Katsnelson, M.I. (2013). Origin of Anomalous Water Permeation through Graphene Oxide Membrane, *Nano letters*, July 19, 13(8), 3930–3935. DOI: 10.1021/nl4020292.

8. Jianchen, Hu, Yanfeng, Ji, Yuanyuan, Shi, Fei, Hui, Huiling, Duan & Mario, Lanza, (2014). A Review on the use of Graphene as a Protective Coating against Corrosion, *Ann. Mater. Science & Engineering,* Vol. 1, Issue 3.

9. Singh, B.P., Nayak, S., Nanda, K., Bikash, K.J., Bhattacharjee, S. & Besra, L. (2013). The production of a corrosion resistant graphene reinforced composite coating on copper by electrophoretic deposition, *Carbon*, Vol. 61, September 2013, Pages 47–56. DOI: 10.1016/j.carbon.2013.04.063.

10. Yao, Tong, Siva, Bohm & Mo, Song, (2013). Graphene based materials and their composites as coatings, *Austin J. Nanomed. & Nanotech.,* Vol. 1 Issue 1.

11. Schriver, M., Regan, W., Gannett, W.J., Zaniewski, A. M., Crommie, M.F. & Zettl, A. (2013). Graphene as a Long--Term Metal Oxidation Barrier: Worse Than Nothing, *ACS Nano,* Vol. 7, No. 7, 5763–5768. DOI: 10.1021/nn4014356.